Spin- and valley-dependent analysis of the two-dimensional low-density electron system in Si MOSFETs

M. W. C. Dharma-wardana* and François Perrot†
Institute of Microstructural Sciences, National Research Council of Canada, Ottawa, Canada K1A 0R6
(Received 25 February 2004; revised manuscript received 26 April 2004; published 16 July 2004)

The two-dimensional electron system (2DES) in Si metal-oxide field-effect transistors consists of two distinct electron fluids interacting with each other. We calculate the total energy as a function of the density n and the spin polarization ζ in the strongly correlated low-density regime, using a classical mapping to a hypernetted-chain (CHNC) equation inclusive of bridge terms. The ten distribution functions arising from spin and valley indices are calculated to obtain the total free energy, the chemical potential, the compressibility, and the spin susceptibility. The $T=0$ results are compared with the two-valley quantum Monte Carlo (QMC) data of Conti and Senatore [Europhys. Lett. **36**, 695 (1996)] (at $T=0$, $\zeta=0$) and found to be in excellent agreement. Unlike in the one-valley 2DES, it is shown that *the unpolarized phase is always the stable phase in the two-valley system*, right up to Wigner crystallization at $r_s \sim 40$. Hence g^* is insensitive to the spin polarization and to the density. The compressibility and the spin-susceptibility enhancement calculated from the free energy validate a simple approach to the two-valley response based on coupled-mode formation. The local-density approximation of density-functional theory is shown to fail, especially near $r_s=1$, even though the 2DES is uniform. The spin-susceptibility enhancement calculated from the coupled-valley response and directly from the two-valley energies is discussed. The three methods, QMC, CHNC, and coupled-mode theory, agree closely. Our results contain no *ad hoc* fit parameters and lead to general agreement with available experimental results.

DOI: 10.1103/PhysRevB.70.035308 PACS number(s): 71.45.Gm, 05.30.Fk, 71.10.−w

I. INTRODUCTION

The two-dimensional electron systems (2DES) in GaAs-like structures, as well as those found in Si metal-oxide field-effect transistors (MOSFETs) access a wide range of electron densities under controlled conditions, providing a wealth of experimental observations.[1] The nature of the physics depends on the "coupling parameter" Γ = (potential energy)/(kinetic energy). The Γ for the 2DES at the density n happens to be equal to the mean-disk radius $r_s=(\pi n)^{-1/2}$ per electron, expressed in effective atomic units that depend on the bandstructure mass m_b and "background" dielectric constant ϵ_b. Thus $\Gamma=r_s$ is used as a small parameter in Fermi-liquid-like perturbation approaches to the 2DES. In this paper r_s is simply the electron-disk radius and the perturbation theory is *not* used. The 2DES in GaAs-like structures will be called a simple 2DES or one-valley 2DES to distinguish it from the two-valley system found in, e.g., Si MOSFETs. The inversion layer adjacent to an oxide layer grown on the Si (001) surface contains two equivalent valleys which host two equivalent electron fluids. Various aspects of such multi-valley systems were studied[2] by Sham and Nakayama, Rasolt *et al.*, and others, mainly in the high-density limit. The simple 2DES is also a two-component system (two spin species), while the two-valley system involves four components and ten pair-distribution functions (PDFs).

In a recent study of the effective mass m^* and the effective Landé-g factor of the 2DES, the Coulomb coupling between the electrons of the two valleys was shown to have a dramatic effect at low densities when the coupling becomes large.[3] In effect, the elementary excitations of the two fluids in the two valleys interact to form coupled modes, giving rise to new effects. It was shown experimentally[4] that m^*g^* rises rapidly with decreasing density in Si MOSFETs, and that this rise is due to a dramatic increase in m^*, independent of the spin polarization, while g^* remains essentially constant. Calculations for the Si system which account for the intervalley Coulomb coupling quantitatively predict[3] the sharp increase in m^*g^*. It was also shown that g^* remained essentially constant, in strong contrast to the behavior found theoretically for the simple one-valley 2DES.[3] The effective mass was also shown to be practically independent of the spin polarization ζ, in excellent agreement with the data of of Shashkin *et al.*[4] for Si MOSFETs. The enhancement of m^*g^* in the one-valley 2DES of GaAs-like systems is found to be dependent on the spin polarization,[5] in strong contrast to the Si MOSFET case. Our calculations[3] show that the physics of the one-valley system is dominated by the presence of a transition to a fully polarized state, which makes g^* increase rapidly with r_s as the transition density is approached. The two-valley system shows *no such transition to the spin-polarized state* and is relatively insensitive to the spin polarization.

The perturbation theory becomes questionable for $r_s>1$. Instead, we use a direct evaluation of the total free energy $F(n,\zeta,T)$. The second derivative of the total free energy F with respect to the spin polarization ζ gives a value for m^*g^* of the two-valley system. This requires the ζ-dependent two-valley energy, which is not yet available from quantum Monte Carlo (QMC) simulations. However, we can evaluate $F(n,\zeta,T)$ using CHNC, and also show that the hypernetted-chain (CHNC) results agree with QMC data (available at $\zeta=0$ and $T=0$). Another approach, which avoids the need for a full four-component calculation is to build up the two-valley

susceptibility by noting that the one-valley energy $F(n,\zeta,T)$ is available at $T=0$ from QMC, and at any $T\neq 0$ from CHNC. The coupling of the excitations in the two valleys can be included in the coupled response function in a standard way. Then we find that the increase in g^* in the GaAs 2DES is associated with the "blow up" of the single-valley spin response, while the behavior of the Si-MOSFET 2DES is related to the properties of the coupled-mode response. The static small-q limit of the spin response function provides the needed χ_s/χ_p.

The objective of this paper is to (i) present $F(n,\zeta)$ data for the two-valley system by a four-component CHNC calculation involving the ten pair distributions that are needed in the two-valley system, and establish the close agreement of the CHNC results with the QMC calculations, and (ii) construct the coupled-mode response functions using the well-established one-valley data, and show that these results are also validated by QMC and full four-component CHNC results. We will not present detailed finite-T calculations (and hence m^* calculations, as detailed in Ref. 3) in this paper, as such calculations would make the paper too long and unwieldy. Also, finite-T data are not presently available from QMC simulations for comparison. A brief account of the CHNC method is given in Sec. II. In Sec. III we discuss the construction of the coupled-mode response functions which use *only the one-valley exchange-correlation data* to obtain the two-valley behavior. The compressibility predicted via the small-q limit of the so constructed coupled-mode response is found to agree very well with that from QMC or the full four-component CHNC calculations. This validates the coupled-mode model used in the calculation (Ref. 3) of the m^*g^* enhancement in Si MOSFETs. The full two-valley energy calculations enable us to examine the usual one-valley local-density approximation (LDA) in Si MOSFETs and the corrections arising from coupled-mode effects. Finally, we discuss the spin-susceptibility enhancement obtained from these calculations, and the question of relating the electron-disk radius r_s used in these calculations to the experimental densities. Although the main thrust of this study is for two-valley systems, we give comparisons with one-valley results, and with suitable experiments.

II. FOUR-COMPONENT CHNC CALCULATIONS FOR THE TWO-VALLEY ELECTRON FLUID

We consider a 2DES in a Si MOSFET at a total density n, with $r_s^2=1/\pi n$, while the density in each valley $v=a$ or b, is taken to be $n_v=n/2$. Hence the r_s parameter in each valley becomes $r_{sv}=r_s\sqrt{2}$. Thus we do not consider density polarizations leading to $n_a\neq n_b$. Also, the electrons in both valleys have the same spin polarization ζ and the same temperature T. This is consistent with recent studies that show that the valley splitting is very slight.[6] If the two spin species are denoted by $i=1,2$, we have a four-component 2DES with ten independent PDFs, viz., $g_{ij,vw}(r)$. We define $k=1,2$ for the two spins in valley a, and $k=3,4$ for the two spins in valley b, and write the PDFs as $g_{kl}(r)$. The CHNC method for 2DES has been described fully in Ref. 7, where the quantum fluid at $T=0$ is considered to be equivalent to the classical fluid at a quantum temperature $T_q(r_s)$. It contains the essential "many-body" input to the problem. In a brief outline, in CHNC we assume that the 2D electrons are mapped onto a classical system where the distribution functions are given by a finite-T classical density functional form,

$$g_{kl}(r)=e^{-\beta\{P(r)\delta_{kl}+V_{cou}(r)+V_c[r:(g_{kl})]\}}. \tag{1}$$

Here, $\beta P(r)$ is a "Pauli exclusion potential," which acts only for parallel spins, i.e, if $k=l$. It is constructed such that $g_{kl}(r)$ becomes identical with the noninteracting PDF, viz., $g^0_{kl}(r)$, which is known from quantum mechanics when the Coulomb interaction $V_{cou}(r)$ and the associated correlation corrections $V_c(r)$ are zero. The Coulomb interaction between two electrons in the equivalent classical picture involves a correction arising from their mutual diffraction effects. Thus $V_{cou}(r)$ is obtained by solving a two-electron Schrodinger equation. The result is parametrized by the form,[7]

$$V_{cou}(r)=(1/r)[1-\exp(-k_{th}r)], \tag{2}$$

$$k_{th}/k_{dB}=1.1587T_{cf}^{0.103}, \tag{3}$$

$$k_{dB}=(2\pi m^*T_{cf})^{1/2},\quad T_{cf}^2=(T_q^2+T^2). \tag{4}$$

Here k_{dB} is the de Broglie momentum of the scattering pair with the effective pair mass $m^*=1/2$, and T_{cf} is the classical fluid temperature which reduces to T_q at $T=0$. The correlation potential $V_c(r)$ occurring in Eq. (1) is taken to be the sum of hypernetted-chain diagrams inclusive of a bridge term. Thus V_c is nonlocal and is a function of the $g_{kl}(r)$, which have to be self-consistently calculated. The bridge term mimics the higher-order correlations which are *not* captured by the simplest HNC equations. These were shown to be important in 2D electron systems in Ref. 7. Particles having identical indices ($k=l$) are restricted from close approach by the Pauli exclusion effect modeled by $P(r)\delta(kl)$. However, singlet pairs of electrons, or electrons in two different valleys, contribute to strong Coulomb correlations, and hence a bridge term is included in all such "off-diagonal" PDFs. The bridge term $B_{kl}(r)$ for $k\neq l$ applies to six different PDFs, and we have taken this to be given by the usual hard-disk functional form discussed in Ref. 7. (Khanh and Totsuji[8] have studied a more detailed implementation of the hard-disk bridge function in CHNC, while Bulutay and Tanatar[9] have studied the 2D CHNC without a bridge correction.) It should be emphasized that both the HNC approximation, as well as the need for a bridge function, can be avoided by using the classical mapping to a quantum fluid (CMQF), where we use classical molecular dynamics (MD) to generate the PDFs of the classical fluid under consideration. In such a scheme we use the pair potential given by Eq. (2), plus the Pauli potential in an MD simulation for a classical plasma at the temperature T_{cf}. Such a CMQF-MD scheme would be numerically more demanding than the CHNC, much simpler than the full QMC simulations, and have the advantage of not making the HNC+bridge approximations. However, the two-valley (four-component) system examined here has been studied by QMC and we use those results to confirm the validity of our methods.

TABLE I. Comparison of the total energy $\epsilon_{tot}(r_s)$ and the correlation energy $\epsilon_c(r_s)$, in atomic units at $T=0, \zeta=0$ for the two-valley 2DES obtained from CHNC, with the QMC data of Conti *et al.* (Ref. 10).

r_s	$\epsilon_{tot}(r_s)^{QMC}$	$\epsilon_{tot}(r_s)^{CHNC}$	$\epsilon_c(r_s)^{QMC}$	$\epsilon_c(r_s)^{CHNC}$
2.0	−0.29302	−0.29172	−0.14315	−0.14202
10.0	−0.08611	−0.08647	−0.04607	−0.04649
20.0	−0.04641	−0.04643	−0.02577	−0.02581
30.0	−0.03196	−0.03183	−0.01806	−0.01795

The main difference in the physics of the one-valley system and the two-valley system arises from the preponderance of direct Coulomb interactions (from six PDFs in the two-valley, and one in the one-valley) over the exchange interactions (from four PDFs in the two-valley, and two in the one-valley). This is the main reason for the lack of a transition to a stable $\zeta=1$ state at low density. Since the transition to a $\zeta=1$ state does not occur as r_s increases, the g^* remains insensitive to increasing r_s, as found theoretically,[3] and experimentally.[4]

The ten coupled equations for $g_{kl}(r)$ are self-consistently solved for many values of the coupling constant λ applied to the Coulomb interaction. Usually seven to 13 values are sufficient, depending on the convergence. The resulting $g_{kl}(r:\lambda)$ are used in the adiabatic connection formula to determine the exchange-correlation free energy of the two-valley 2DES. While our calculations are easily carried out for any value of ζ, T, and r_s, the four-component QMC calculations at finite T,ζ are a major computational undertaking which has not been attempted. However, at $T=0, \zeta=0$, Conti and Senatore[10] have presented QMC results for 2D electron bilayers separated by a distance d_L. They give total energies and also a fit to the correlation energy/electron $\epsilon_c(r_s,\zeta=0,T=0)$ at $d_L=0$, i.e, the case where both electron gases reside in the same layer. In Table I we compare the four-component CHNC with the available four-component QMC data at $d_L=0$. The energies $\epsilon_c(r_s)^{QMC}$ are from the Rapisarda-Senatore fit formula[11] with the parameters quoted in Table I of Ref. 10.

These results show that the CHNC method provides a simple and accurate approach to the treatment of exchange and correlation in the four-component system. In situations where QMC results are available for the correlation energies, we adopt the QMC parametrizations. Thus one may use the parametrization of ϵ_c given by Conti and Senatore for the $T=0, \zeta=0$ case. For $r_s>1$ applications, the Tanatar-Ceperley[12] form may also be used for parametrizing the two-valley system as well, with the parameter values $a_0=-0.40242$, $a_1=1.1319$, $a_2=1.3945$, and $a_3=0.67883$ fitted to a database from $r_s=1$ to 30.

The $T=0, \zeta=1$ case is particularly interesting, since this system (i.e, a two-valley system at density n) is mathematically identical to the one-valley system at the same density, but with $\zeta=0$, for the Hamiltonian considered by Conti and Senatore, and by us in this study. In this case the two-valley system has a twofold symmetry since the energy is the same, irrespective of the orientation of the spin in each valley. That is, $\zeta=1$ means all the spins in valley *a* are oriented, while all the spins in valley *b* are also oriented, but independently of the orientation of the spins in *a*. This degeneracy would be resolved in real Si MOSFETs, but not in the model used here, or in Conti and Senatore. For instance, the three-body correlations for intervalley interactions may be slightly different from those in the *intra*valley interactions, and hence may require two different bridge parameters, to be determined variationally by an energy minimization using the hard-disk reference fluid approach. We have not done this, and simply used the same bridge parameter as in Ref. 7 for all interactions. In the QMC calculation this would require independent optimization of the model for back-flow corrections. Finally, the correlation energy of the fully spin-polarized (degenerate) two-valley system can be parametrized using the Tanatar-Ceperley form with $a_0=-0.19162$, $a_1=3.6123$, $a_2=1.9936$, and $a_3=1.4714$ in atomic units.

TABLE II. The correlation energy $\epsilon_c(r_s,\zeta)$ per electron, as a function of ζ, estimated using the one-valley polarization factor of Eq. (5), and from the full two-valley CHNC calculation.

r_s	ϵ_c^{fit}	ϵ_c^{CHNC}	ϵ_c^{fit}	ϵ_c^{CHNC}
$\zeta\rightarrow$	0.25	0.25	0.75	0.75
5.0	−0.07686	−0.07757	−0.06286	−0.06434
10.0	−0.04518	−0.04562	−0.03765	−0.03831
20.0	−0.02529	−0.02535	−0.02134	−0.02151
30.0	−0.01772	−0.01764	−0.01477	−0.01504

A. The energy of unpolarized and polarized phases

The $T=0$ correlation energy at finite values of ζ were calculated using the CHNC procedure and compared with the values predicted from the polarization factor used for the one-valley 2DES. This has the form[7]

$$p(r_s,\zeta)=\frac{\epsilon_c(r_s,\zeta)-\epsilon_c(r_s,0)}{\epsilon_c(r_s,1)-\epsilon_c(r_s,0)}=\frac{\zeta_+^{\alpha(r_s)}+\zeta_-^{\alpha(r_s)}-2}{2^{\alpha(r_s)}-2},$$

$$\alpha(r_s)=C_1-C_2/r_s+C_3/r_s^{2/3}-C_4/r_s^{1/3}. \quad (5)$$

Here, $\zeta_\pm=(1\pm\zeta)$. It turns out that the coefficients C_1-C_4 obtained for the one-valley 2DES, i.e., 1.5404, 0.030544, 0.29621, and 0.23905, respectively, work quite well for the two-valley system as well, even at high r_s. Thus, using the TC-type fit formula for the two-valley $\epsilon_c(r_s,\zeta=1)$ and $\epsilon_c(r_s,\zeta=0)$, the estimated values of $\epsilon_c(r_s,\zeta)$ and the CHNC values are given in Table II. Our spin-dependent function respects the Hartree-Fock limit. Attaccalite *et al.*[20] have given a functional representation for 2D spin-polarized systems, where they have attempted to carefully respect the high-density and low-density behaviors of the *xc* energy. We find that their parametrization could also be adapted to the present problem.

The finite-ζ calculations show that there is *no ferromagnetic phase transition* in this system at $T=0$, since the total energy of the $\zeta=0$ phase is always more negative than any polarized phase. This is expected from the dominance of the

TABLE III. Comparison of the exchange-correlation energy $\epsilon_{xc}(r_s)$ per electron, and the Kohn-Sham potential $V_{xc}(r_s)$, in atomic units at $T=0, \zeta=0$ for the two-valley 2DES obtained from QMC fit or CHNC, and from the LDA.

r_s	$\epsilon_{xc}(r_s)^{LDA}$	$\epsilon_{xc}(r_s)^{QMC}$	$V_{xc}(r_s)^{LDA}$	$V_{xc}(r_s)^{QMC}$
1.0	−0.70960	−0.62843	−1.02897	−0.88608
2.0	−0.38213	−0.35535	−0.55189	−0.50271
10.0	−0.09007	−0.08851	−0.13133	−0.12835
20.0	−0.04742	−0.04699	−0.06957	−0.06874

many off-diagonal terms contributing to direct Coulomb interactions, but without exchange interactions. This was pointed out in Ref. 3, where the insensitivity of m^*g^* to ζ obtained from the theory was in excellent agreement with the experiments of Shashkin *et al.*[4] The stabilization energy ΔE of the $\zeta=0$ phase with respect to the fully polarized phase is 0.12734×10^{-3} a.u. at $r_s=25$, and diminishes to 0.89929×10^{-4} a.u. at $r_s=40$. These are very small energy differences and within the error of the CHNC method, and possibly of the two-valley QMC calculations. However, the pattern of stability of the $\zeta=0$ phase holds for all r_s investigated. We arrive at the conclusion: *there is no spin-phase transition in the two-valley system*.[13]

B. LDA-type calculations for Si MOSFETs

In most density-functional calculations of Si/SiO_2 quantum wells, the Kohn-Sham exchange-correlation (xc) potential $V_{xc}(r)$ is calculated using the LDA, where the total density $n(r)$ is considered without taking account of the valley degeneracy. In effect, the electron gas is assumed to be a *single* electron gas at a density r_s and its exchange-correlation energy $\epsilon_{xc}(r_s)$ and the Kohn-Sham potential $V_{xc}(r_s)$ are calculated at the given density. [We recall that $V_{xc}(r_s)$ is simply the xc contribution to the chemical potential μ_{xc}.] Results for ϵ_{xc} and μ_{xc} for electrons in a Si MOSFET calculated correctly, i.e., taking account its degenerate valley structure, and in the usual LDA approach, are compared in Table III. The full chemical potential μ, as well as the compressibility ratio K^0/K calculated for the two-valley system, and that obtained within the LDA approach, are also shown in Fig. 1. It is noteworthy that the total chemical potential has a minimum near $r_{sm}\sim1$. In effect, a low-density electron fluid ($r_s>r_{sm}$) whose chemical potential is equal to that of a high-density gas ($r_s<r_{sm}$) exists and this could lead to spontaneous density inhomogeneities in these systems.

When the actual electron densities in Si MOSFETs are converted to effective r_s units (see below), the r_s range 1–6 is the most important for device applications, and hence, overestimates in V_{xc} contained in the usual LDA approach could be significant. This becomes even more significant in spin-density functional applications to Si-based nanostructures.

C. Pair-distribution functions in the Si-MOSFET system

The PDFs, denoted by $g_{kl}(r)$, embody the detailed particle correlations in the system. In Fig. 2 we display an illustrative

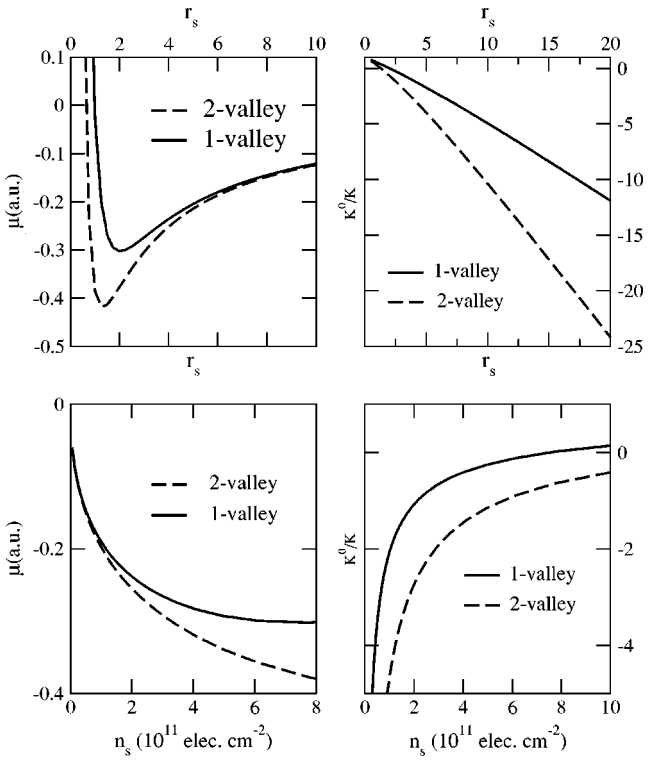

FIG. 1. Left panels: Comparison of the total chemical potential μ, i.e, the total Kohn-Sham potential, calculated at the total density n and r_s, for the two-valley system, and if the LDA were used (labeled 1-valley), ignoring the two-valley nature. Right panels: Same for the compressibility ratio.

set of pair-distribution functions. QMC-based PDFs have not been reported in the literature and hence we do not have a direct comparison. However, good agreement between CHNC and QMC-based PDFs have been found in other systems (e.g, 2DES, 3DES, and fluid hydrogen).[7,14–16] For $\zeta=0$ the four diagonal PDFs g_{kk} are identical, and similarly, all of the six off-diagonal PDFs are also identical. Hence there are actually only two distinct PDFs, just as in the single-valley case, where g_{11} and g_{12} define the $\zeta=0$ case. These are shown for $r_s=2$, 10, and 20 in the top panel of Fig. 2. It is also clear that the correlation effects are mainly determined by the off-diagonal PDFs. This is in keeping with our understanding that singlet-like correlations are more important than parallel spin (ferromagnetic) correlations in the two-valley system. At finite ζ there are five independent PDFs. There are two independent diagonal PDFs, $g_{11}=g_{33}$ and $g_{22}=g_{44}$. The three independent off-diagonals are $g_{12}=g_{23}=g_{34}=g_{14}$, g_{13}, and g_{24}. These are shown for the case $r_s=10$ and $\zeta=0.5$ in the lower panel of Fig. 2.

III. RESPONSE FUNCTIONS

In the following we discuss the linear response functions, since the static small-k limit can be related to the derivatives of the total energies that were calculated from CHNC or QMC, if available. This enables us to verify a simple procedure for the construction of the two-valley response functions using *only* single-valley exchange correlation data.[3]

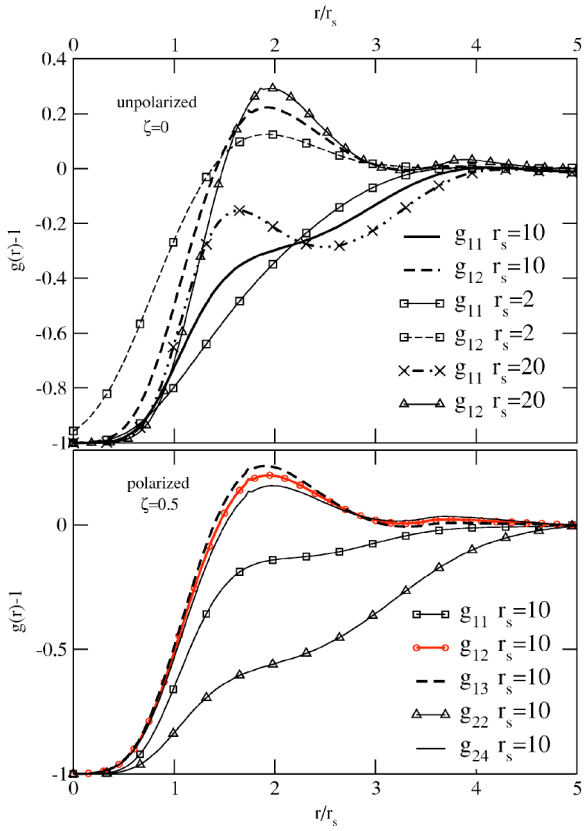

FIG. 2. Pair-distribution functions (PDFS) of the two-valley system. For $\zeta=0$ the ten PDFs reduce to two independent PDFs. The top panel gives this case for $r_s=2,10$, and 20. For $\zeta\neq 0$ there are five independent PDFs. These are shown for $r_s=10$.

The density-density response function $\chi(k,\omega)$ will be called the *d-d* response for brevity. We emphasize that this is not a "fluctuation" analysis, but a strictly thermodynamic approach based on the small-k limit of the static response functions, as discussed below.

The response function is expressed in terms of a reference "zero-order" $\chi_R^0(k,\omega)$ and a local-field factor (LFF), denoted by $G(k,\omega)$.

$$\chi(k,\omega)=\chi_R^0(k,\omega)/[1-V_k\{1-G_d(k,\omega)\}\chi_R^0(k,\omega)]. \quad (6)$$

The *s-s* response (or "spin susceptibility") is written as

$$\chi_s(k,\omega)=-\mu_B^2\chi_R^0(k,\omega)/[1-V_k\{1-G_s(k,\omega)\}\chi_R^0(k,\omega)], \quad (7)$$

where μ_B is the Bohr magneton. Note that our definition of the spin LFF differs somewhat from a commonly used definition.[17] Our form makes the *d-d* and *s-s* LFFs appear formally similar, at least at this stage. Hence, a single discussion applies to both, and we drop the subscripts *d* and *s*. The reference function $\chi_R^0(k,\omega)$ has the form

$$\chi_R^0(k,\omega)=\sum_{\vec{k},\sigma}\frac{n_{\sigma,\vec{k}}-n_{\sigma,\vec{k}+\vec{q}}}{\omega+\epsilon_{\vec{k}}-\epsilon_{\vec{k}+\vec{q}}}. \quad (8)$$

Here $\vec{k},\vec{q}$ are two-dimensional vectors, while the corresponding single-particle energies are denoted by $\epsilon_{\vec{k}}$, etc. The Fermi occupation number $n_{\sigma,\vec{k}}$ may be chosen to be the noninteracting value, in which case χ^0 is the 2D Lindhard function.[2] An alternative is to use the fully interacting density, evaluated from the fully interacting chemical potential, as in the density-functional theory (DFT).

The small-k limits of the local-field factors $G_d(k,\omega)$ and $G_s(k,\omega)$ can be obtained from the second derivatives of the exchange-correlation free-energy functional $F_{xc}(n,\zeta)$ of DFT, with respect to the charge densities or the spin densities.[18] These second-order derivatives, together with the second derivative of $F_{xc}(n,\zeta)$ with respect to T for a two-valley system, were used in our m^* and g^* calculations reported in Ref. 3, using the CHNC technique. Here we look at the compressibility and spin susceptibility of the two-valley system obtained from the small-k limit of the coupled-mode response function (built up from one-valley data) and compare it with that obtained directly from the two-valley CHNC and QMC.

A. Response functions of the two-valley system

The theory of the one-valley fluid can be used for the two-valley (four-component) fluid if there is no valley polarization (i.e., the two valleys are assumed equivalent although distinct), as in Ref. 3. As this may not be completely clear from the abbreviated discussion in Ref. 3, we present some details here.

In the theory of classical fluids, the response functions are simply related to the structure factors, while the LFFs are simply related to the direct correlation functions of Ornstein-Zernike (OZ) theory. Since this paper is directed more towards electron-fluid studies, we follow the language of the LFFs and the related response methodology, rather than the OZ presentation.

Let us indicate the species (which may be a valley index or a spin index) by u or v, taking the values 1 and 2, and consider a weak external potential $\phi_v(\vec{k},\omega)$ that acts only on the electrons of species v. The external potential induces density deviations $\delta n_v(\vec{k},\omega)$ such that:[19]

$$\delta n_u(\vec{k},\omega)=\sum_v \chi_{uv}(\vec{k},\omega)i\phi_v(\vec{k},\omega). \quad (9)$$

These equations define the linear *d-d* response functions involving the species u and v. The longitudinal dielectric function $\varepsilon(\vec{k},\omega)$ is now given by

$$1/\varepsilon(\vec{k},\omega)=1+V_k\sum_{u,v}\chi_{uv}(\vec{k},\omega). \quad (10)$$

Here V_k is the 2D Coulomb interaction $2\pi/k$. Note that we are using effective atomic units (Hartrees, etc.), such that e^2 divided by the background dielectric constant is taken to be unity (see Sec. IV). To relate the response functions to the

local fields, we consider the effective potentials $U_v(\vec{k},\omega)$ such that

$$U_v(\vec{k},\omega) = V_k[1 - G_{uv}(\vec{k},\omega)]\delta n_v(\vec{k},\omega). \tag{11}$$

Thus the bare Coulomb interaction between the particles of type u and v is modified by the LFFs G_{uv}. Hence, we can write the density deviations $\delta n_u(\vec{k},\omega)$ in terms of the effective potentials and the zeroth-order response functions as follows (we drop the $\vec{k},\omega$ labels for brevity):

$$\delta n_u = \chi_u^0\left[\phi_u + V_k\sum_v (1 - G_{uv})\,\delta n_v\right]. \tag{12}$$

Now, by a comparison of the Eqs. (9) and (12), we can write down the response functions of the coupled two-component system in terms of the zeroth-order response functions and the LFFs.

$$\chi_{11} = \chi_1^0\, d_2/D, \quad \chi_{22} = \chi_2^0\, d_1/D, \tag{13}$$

$$\chi_{12} = V_k\chi_1^0\chi_2^0[1 - G_{12}]/D, \tag{14}$$

$$d_1 = 1 - V_k\chi_1^0[1 - G_{11}], \tag{15}$$

$$d_{12} = V_k\chi_1^0[1 - G_{12}], \tag{16}$$

$$D = d_1d_2 - d_{12}d_{21}. \tag{17}$$

We have suppressed the $\vec{k},\omega$ dependence in the above equations, and also not explicitly given χ_{21}, d_2, and d_{21} for brevity. We now define a total coupled-mode response function $\chi_T(\vec{k},\omega)$ via

$$1/\varepsilon(\vec{k},\omega) = 1 + V_k\chi_T(\vec{k},\omega). \tag{18}$$

Then the total two-component 2DES response is given by

$$\chi_T = [\chi_1^0 + \chi_2^0 + V_k\chi_1^0\chi_2^0G_\Sigma]/D, \tag{19}$$

$$G_\Sigma = G_{11} + G_{22} - G_{12} - G_{21}. \tag{20}$$

The evaluation of χ_T using *only one-valley xc-data* is our objective. In the following, we sometimes denote χ_T by χ_{cm} to emphasize the coupled-mode nature of the total response. If we are dealing with a simple (one-valley) electron fluid, e.g., a partially spin-polarized electron gas, the species index v is simply the spin index. Notice that the coupling between the two systems (be they spins or valleys) replaces the individual denominators d_1 and d_2 by a new denominator D, common to both systems, and containing the cross terms d_{ij}. That is, instead of the two sets of excitations given by the zeros of d_1 and d_2, we now have a *common set of "coupled-mode" excitations* defined by the zeros of D. We emphasize that in this analysis we have *not* used any form of CHNC theory.

All the response functions prior to the switching on of the Coulomb interaction between the two valleys are known. The problem is to determine the cross terms d_{ij}, i.e, the intervalley term, d_{uv}, occurring in the coupled-mode denominator D, using only the free-energy data for a single valley. If we consider the small-k limit, we see that the terms d_{ij} occurring in D are directly related to the second-density derivative or magnetization derivative of the free-energy contributions F_{ij} arising from the PDFs g_{ij}. We know these *individual* free-energy contributions for the one-valley problem.

Let us first consider the small-k limit of the static response functions to make contact with the compressibility and susceptibility sum rules.

B. Small-k limit of the static response

The small-k behavior of the static response is related to the second derivative with respect to the density (or magnetization), and this provides well-known sum rules that we exploit here. For simplicity, and for comparison with the degenerate two-valley case, let us review the one-valley paramagnetic case $\zeta=0$, and consider the calculation[3] of the small-k, static ($\omega=0$) limit of the simple (one-valley) response function,

$$\chi_v(n_v) = \chi^0(n_v)/[1 - V_k(1 - G_{vv})\chi^0(n_v)]. \tag{21}$$

The density-density response function is associated with the proper polarization function Π_v. Dropping the species subscript v for the present, we have

$$\Pi = \Pi^0/(1 + V_kG\Pi^0), \tag{22}$$

$$\Pi^0 = -\chi^0. \tag{23}$$

The small-k behavior of this function states that

$$\Pi/\Pi_0 = \kappa/\kappa_0. \tag{24}$$

The compressibility κ is calculated via the chemical potential μ, starting from the total free energy per unit volume obtained from the CHNC calculation.

$$F = F_0 + F_x + F_c, \tag{25}$$

$$F = \sum_v n_v[\epsilon_0^v(n_v) + \epsilon_x^v(n_v)] + n\epsilon_c(n), \tag{26}$$

$$\epsilon_0^v = (1 + \zeta^2)/2r_{sv}^2, \tag{27}$$

$$\epsilon_x^v = -\frac{2\sqrt{2}}{3\pi r_{sv}}[(1 + \zeta)^{3/2} + (1 - \zeta)^{3/2}], \tag{28}$$

$$\mu = \frac{dF}{dn} = \mu_0 + \mu_x + \mu_c, \tag{29}$$

$$1/\kappa = n^2\frac{d\mu}{dn}. \tag{30}$$

At $T=0$, the chemical potential is given (in Hartrees) by

$$\mu = n_v\pi - 2(2/\pi)^{1/2}n_v^{1/2} + \mu_c. \tag{31}$$

The compressibility calculated directly from the four-component calculation should agree with that obtained from the coupled-valley formalism. There, the small-k limit of the

denominator of the density-density proper-polarization function is given by

$$1 + V_k G_d \chi^0 = \kappa/\kappa_0.$$

Here G_d is the LFF of the density-density polarization function. Hence the denominator d_1, or d_2 of the *d-d* response occurring in Eq. (13), for any particular species is available for the density-density response function in each valley. But the cross density-density LFFs, e.g., G_{12}, and the cross-denominators d_{12} needed to form the coupled-valley forms are not yet specified.

In the case of the spin susceptibility χ_s, the role played by the compressibility is taken over by the spin stiffness, which is the second derivative of the free energy F with respect to the spin polarization ζ. Here we have, for a single valley,

$$\chi_s/\chi_P = 1 + d^2\{r_{sv}^2 F_{xc}\}/d\zeta^2. \tag{32}$$

Hence the denominators d_u and d_v of the spin susceptibilities of both 2DES are known, at the valley densities $n_v = n_u = n/2$, from a simple CHNC calculation or from a QMC energy parametrization. However, here again the cross terms d_{12} and d_{21} (which are equal) needed to complete the calculation of the coupled susceptibility [Eqs. (13) and (19)] are not yet specified.

The cross term for the *d-d* response, or for the *s-s* response, can be calculated if the free-energy contribution F_{uv} arising from the Coulomb interaction among the electrons in the two valleys is known. The interaction is among the electrons of valley u, at density $n/2$, and the electrons of valley v at density $n/2$. The intervalley free-energy contribution $F_{uv}(n/2, n/2)$ is purely Coulombic, and hence, it is clearly analogous to the correlation free-energy term arising from the antiparallel-spin PDF, i.e., $g_{12}(n, \zeta=0)$ of the simple one-valley 2DES *at density n* with two spin species. The case $\zeta = 0$ ensures that the total density is split as $n_u = n_v = n/2$. Thus the d_{12} term needed for the spin-susceptibility calculation and the density-density response calculations are

$$s - s\ d_{12} = d^2\{r_s^2 F_c[g_{12}]\}/d\zeta^2, \tag{33}$$

$$d - d\ d_{12} = -(2/\pi) d^2 F_c[g_{12}]/dn^2. \tag{34}$$

Note that d_1 is calculated from $F_{xc}(n/2, \zeta=0)$, while d_{12} is from $F_c(n, \zeta=0)$ of the simple one-valley 2DES. Hence, knowing d_1, d_{12} (which are equal to d_2 and d_{21}, since the valleys are degenerate), we can calculate the susceptibility enhancement χ_s/χ_P, as well as the compressibility ratio κ/κ_0 of the interacting two-valley 2DES, without actually solving the coupled system of ten distribution functions needed in the full CHNC calculation of the four-component system.

1. Results for the compressibility ratio and the susceptibility ratio

We consider the compressibility ratio K_0/K obtained by the coupled-mode analysis and from the two-valley QMC data,[10] or equivalently, from the four-component CHNC data, in Fig. 3. The excellent agreement shows that the coupled-mode procedure for using the one-valley data to generate two-valley data is successful.

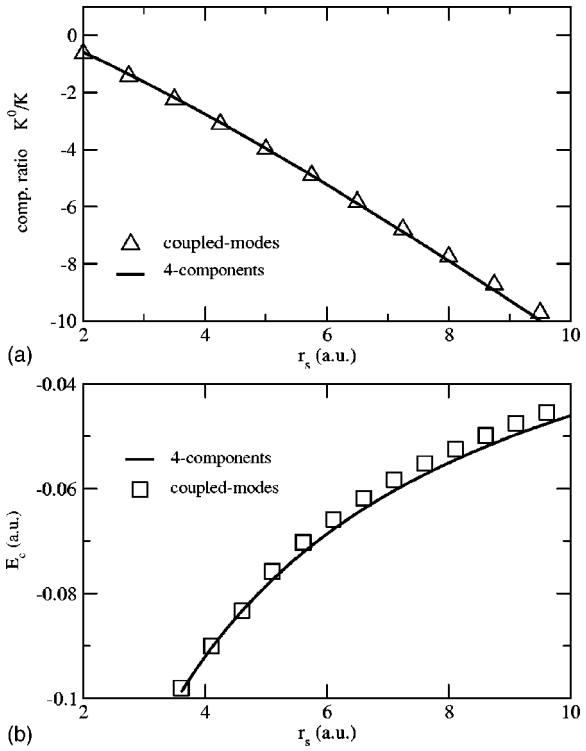

FIG. 3. (a) Comparison of the compressibility ratio $\Pi_0/\Pi_{cm} = K^0/K$ obtained from the coupled-mode approach, and from the second-density derivative of the total free energy of the four-component system. (b) The energy estimate $\epsilon_c(rs, \zeta=0)$ from the coupled-mode form and from the four-component QMC (Ref. 10).

The calculation of the susceptibility enhancement was given briefly in Ref. 3. We consider the susceptibility enhancement in more detail. Equation (32) involves the second ζ derivative of the correlation energy. It is well known that the ζ-dependent QMC calculations are more prone to errors, since a whole shell of spins need to be reversed. In fact, the one-valley 2DES calculations of Rapisarda and Senatore[11] using diffusion Monte Carlo (DMC) predict a value of $r_s \sim 20$ for the spin transition, different from that ($r_s \sim 26$) predicted by Attaccalite *et al.*,[20] who also use very similar DMC methods. This difference may be due to improvements in computers and techniques. It is also partly an indication of the type of uncertainty that may be had in QMC calculations. QMC simulates a finite system of N electrons with periodic boundary conditions corresponding to closed-shell configurations. This means that only some N are "good" and, once N is fixed, only some values of ζ are allowed. Changing N, the possible values of ζ change. Thus, one has to perform the extrapolation to infinite N *and at the same time* construct an analytic fit to the ζ dependence. No ζ-dependent QMC data are as yet available for the two-valley system. Using Eq. (5) we can write an *approximate* explicit form at $T=0$,

$$\epsilon_c(r_s, \zeta) = \epsilon_c(r_s, 0) + [\epsilon_c(r_s, 1) - \epsilon_c(r_s, 0)] p(r_s, \zeta),$$

$$\frac{d^2\epsilon_c(r_s, \zeta)}{d\zeta^2} = \Delta E(1,0) \frac{d^2 p(r_s, \zeta)}{d\zeta^2}.$$

Thus the energy difference between the polarized and unpolarized phases appears directly. This becomes zero in systems

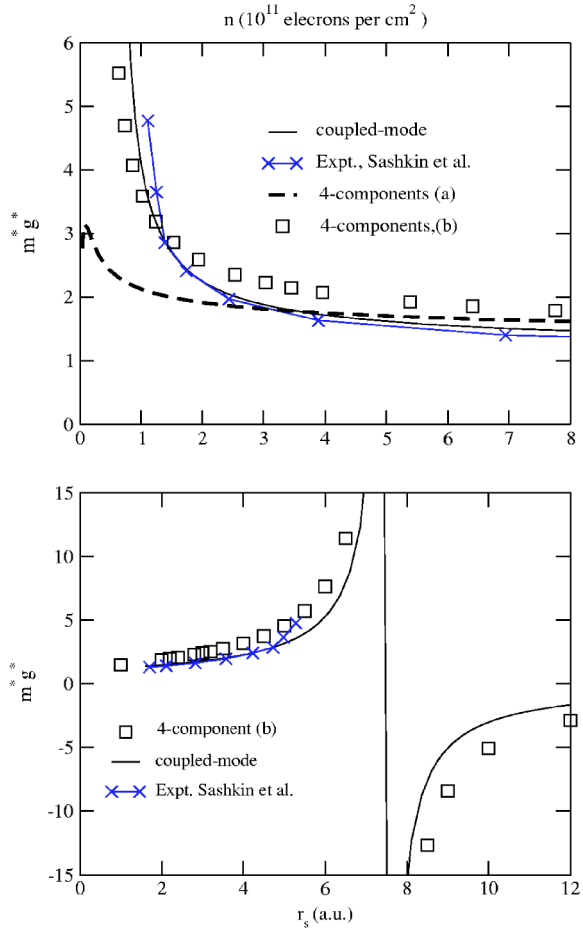

FIG. 4. Comparison of the susceptibility enhancement $\chi_{cm}/\chi_P = m^*g^*$ obtained from the coupled-mode approach and from the second ζ derivative of the total free energy of the 4-component system. The curves marked "4-components" (a), (b) differ by ~5% in the value of the second ζ derivative of the correlation energy, showing the strong sensitivity to this energy derivative.

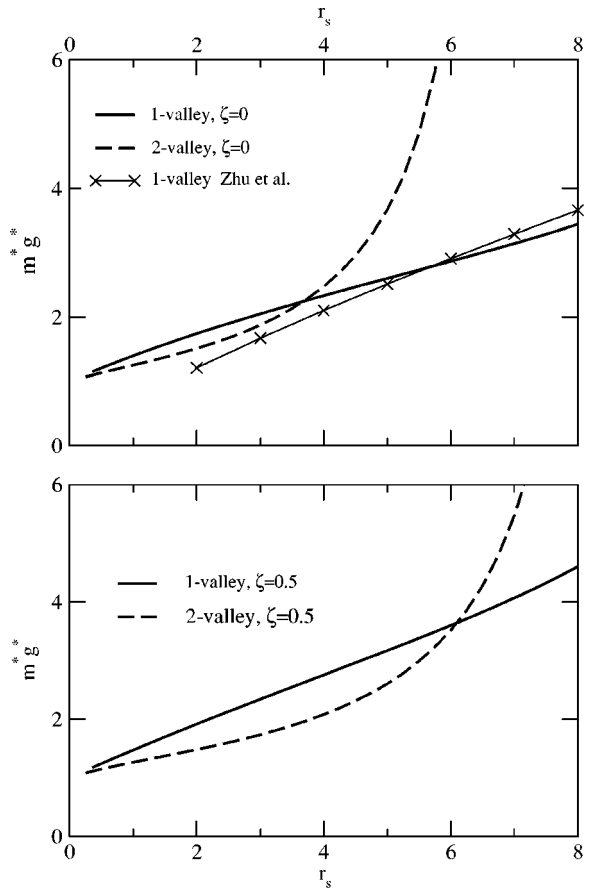

FIG. 5. Comparison of the susceptibility enhancement $\chi_{cm}/\chi_P = m^*g^*$ if a given total electron density is assumed to be entirely in a one-valley 2DES, or equally divided to form a two-valley 2DES. Here, ζ is the spin polarization. The experimental data of Zhu *et al.* for the one-valley GaAs 2DES are also shown.

like the one-valley 2DES that show a spin transition. Even in the two-valley system, where there is no transition to a stable $\zeta=1$ state, we can expect the calculated χ_s/χ_P or χ_{cm}/χ_P to be quite sensitive to $\Delta E(1,0)$, and to the details of the form of the ζ-dependent function. We find that this is very much the case. In Fig. 4 we display the coupled-mode evaluation of $m^*g^*=\chi_{cm}/\chi_P$, with the value of χ_s/χ_P obtained from the ζ-second derivative of the energy obtained from the full four-component calculation. We give curves labeled "four-component" (a), and (b), where the contribution from the $d^2\epsilon_c/d\zeta^2$-derivative term differs by ~5%. Clearly, this small change has a drastic effect on the m^*g^* evaluation. We have also included the experimental results of Sashkin *et al.* for m^*g^* to show that the coupled-mode result, which differs slightly (see Fig. 3) from the full four-component result, is actually in close agreement with the experiment. In the lower panel of Fig. 3 we compare the two-valley correlation energy $\epsilon_c(r_s,\zeta=0)$ from the coupled-mode analysis and from the direct four-component QMC calculation. As expected, a small difference appears at low densities. This type of error is quite within the errors that are possible in the four-component QMC or the four-component CHNC, and in fitting to the polarization dependence of the numerically calculated correlation energies. We find that the coupled-mode approach, which involves a particular set of numerical (and model) approximations, happens to give the best agreement with Sashkin's experiments, while the four-component CHNC calculation has a different set of numerical approximations and captures the coupled-mode formation via the OZ equations. These results imply that the simple ideal two-valley 2DES quite closely models the experimental Si-MOSFET samples, even though any actual differences in the two valleys, the effect of impurities, etc., are not included in the theory.

Coupled-mode formation implies that the excitation spectrum of the system no longer shows the features of the individual valleys, and hence is consistent with the conclusions of Ref. 6, where no evidence for intervalley scattering was seen. In this context, it is interesting to compare the spin-susceptibility enhancement if the two-valley nature of the 2DES is ignored and treated as if it were a one-valley system. This is shown in Fig. 5. This figure shows that there are some ranges of density and ζ where the susceptibility ratio decreases if the one-valley system could be switched to a two-valley system.[21] However, for $\zeta=0$ and 0.5 we see that

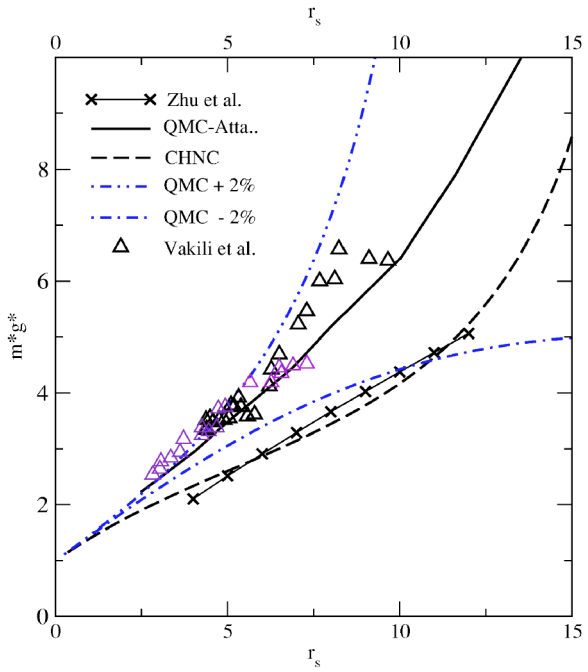

FIG. 6. Comparison of the theoretical susceptibility enhancement $\chi_{cm}/\chi_P = m^*g^*$ for a one-valley system with experimental results. The spin-polarization $\zeta=0$. The effect of a 2% error in the exchange-correlation term [Eq. (35)] on the theoretical $m*g*$ is shown as QMC ±2%.

the two-valley m^*g^* exceeds the one-valley m^*g^* at sufficiently high r_s.

A quantitative comparison with the experimental results of Shkolnikov *et al.* for one-valley systems "switched" to a two-valley system in AlAs is not yet possible. For this, the ellipticity in the Fermi disk in the AlAs 2DES, and the layer thickness, have to be taken into account. However, in the upper figure ($\zeta=0$) we have given a comparison of the CHNC-calculated m^*g^* with the one-valley experimental results of Zhu *et al.*.[5] Here we have used their parametrized formula for $\zeta=0$. The excellent agreement is somewhat fortuitous, since corrections for layer thickness and impurity effects are not included in the theory. An even more important aspect of the comparisons between theory and experiment is shown in Fig. 6, where we look at the experimental data of Zhu *et al.*, the more recent data of Vakili *et al.*,[22] and several predictions of $m*g*$. It is seen that the experimental data of Vakili *et al.* are in quite good agreement with the QMC data[20] of Attaccalite *et al.* However, the correction to the *xc*-susceptibility enhancement arises via the term,

$$\Delta(m^*g^*) = d^2\{(r_s)^2F_{xc}\}/d\zeta^2. \tag{35}$$

This term contains an r_s^2 and also the second-polarization derivative of the *xc* energy. It becomes very sensitive to the errors in assigning r_s as well as to the estimate of the stabilization energy of the unpolarized phase with respect to the polarized phase. The issue of assigning an r_s value to a given 2D density is discussed in Sec. IV. In Fig. 6 we have considered a ±2% deviation in $\Delta(m^*g^*)$ and shown two new estimates. This shows that the Zhu data also fall into agreement with the Attaccalite data, as well as the CHNC theory, for the range $3<r_s<10$. We also note that the CHNC method is based on the use of a quantum temperature T_q fitted to the polarized 2D energies of Tanatar and Ceperley, rather than to the recent Attaccalite data. All this suggests that impurity and layer thickness effects, as well as the theoretical uncertainty in $\Delta(m^*g^*)$, lead to a "fan of uncertainty" of about 2%–3% in the estimate of m^*g^*. The width of the "fan" increases with r_s. We also remark that $\Delta(m^*g^*)$ is divergent for $\zeta=1$. That is, the ease of polarizing the spins (the susceptibility) increases with the degree of polarization and becomes infinite at $\zeta=1$. Hence, experimental results for higher values of ζ would be even more sensitive to various quenching effects which are not included in the idealized theory.

IV. RELATION BETWEEN DENSITY *n* AND THE r_s PARAMETER IN Si MOSFETs

In the 2DES of GaAs/AlAs-type structures, the dielectric constants of the two materials are nearly identical. The lattice constants are also well matched and hence the calculation of the effective atomic units needed in converting the experimental density n to the effective electron-disk radius (r_s) can be carried out in an unambiguous, transparent way. This is important, since the many-body theory is formulated within the language of r_s and effective atomic units. Of course, if the electron gas is not ideally thin, the 2DES becomes a 3D slab and further corrections are necessary.

Unlike in GaAs, the situation for Si MOSFETs is more complicated. The lattice mismatch between crystalline Si and most crystalline varieties (e.g., crystobalite) of SiO_2 turns out to be 35%–40%. The dielectric constants are also strongly mismatched, being ~11.5 and ~3.9 for Si and SiO_2. The large lattice mismatch ensures that there is *no* sharp Si/SiO_2 interface. The reconstruction of the Si atomic layers between the crystalline Si and the SiO_2 bulklike region still contains tetrahedral-bonding networks, but with strongly modified bond angles, bond lengths, etc., characteristic of the amorphization of the Si layers immediately adjacent to the oxide layer. Many decades of experimental and theoretical work have gone into sharpening our understanding of this interface. More recently, first-principles density-functional calculations by Carrier *et al.*,[23] starting from tight-binding models,[24] have presented a clearer picture of the atomic arrangements near the interface region. A series of similar studies by Pasquerello *et al.*[25] establish the geometry of the Si/SiO_2/vacuum interface. Thus, a reliable atomic model of the Si/SiO_2 interface obtained via geometry optimization of the total energy is now available.[23] The essential point is that the Si/SiO_2 interface contains approximately five regions containing crystalline Si (*c*-Si), amorphized Si (*a*-Si), suboxide layers, amorphized silicon dioxide (*a*-SiO_2), and crystalline SiO_2. These are indicated schematically as,

$$[001](z\rightarrow)|c\text{-Si}|a\text{-Si}|\text{suboxides}|a\text{-SiO}_2|c\text{-SiO}_2|. \tag{36}$$

The amorphous (or bond distorted) regions of *a*-Si should be considered as the true insulator that separates the 2DES that reside at the interface between *c*-Si and *a*-Si. Let the location of this amorphization edge be at $z=z_a$. This edge can be

defined to within a few atomic planes within the first-principles theoretical models (see Ref. 23 for more details). If we are dealing with a thick electron gas, then envelope-function methods for describing the form factor may be reasonable. Otherwise, a more detailed atomic description involving Bloch functions is needed. In any case, if the electron gas is very thin, its growth-direction density profile may be considered to be $\delta(z-z_a)$. That is, crystalline Si and *a*-Si flank the two sides of the 2D electron layer, with *a*-Si playing the role of the insulator. The valence bonds of the *a*-Si still form a quasirandom tetrahedral network, even though distorted, and hence the "background" dielectric constant of *a*-Si, is essentially that of Si. That is, the effective dielectric constant,

$$\bar{\epsilon} = 0.5(\epsilon_{si} + \epsilon_{ins}), \tag{37}$$

often used for the 2DES in the MOSFET positioned at an abrupt Si/SiO_2 interface, ignores the effect of the strong lattice mismatch of $\sim 35\% - 40\%$. The second formula of Ando *et al.* (see Appendix of Ref. 2) for the conversion n to r_s, using a mean $\bar{\epsilon}$ of 7.7, is not recommended. Instead, the first formula of Ref. 2, i.e.,

$$r_s/a^* = 1.751\left[\frac{10^{12}\ \mathrm{cm}^{-2}}{n_s}\right]^{1/2}\left[\frac{11.5}{\epsilon_{sc}}\right]\left[\frac{m}{0.19m_0}\right], \tag{38}$$

is clearly the one consistent with the first-principles atomic structure of the Si/SiO_2 interface referred to above.[23] If we look at the Si-MOSFET literature, we find that the formula which uses the average dielectric constant of 7.7, valid for the abrupt Si/SiO_2 interface, has been used by a number of authors. These authors use a value of r_s increased by a factor of ~ 1.49 compared to what we recommend. Thus, Pudalov *et al.*[26] and Okamoto *et al.*[27] have used the mean dielectric constant of 7.7 for their calculation of r_s. However, both these studies use the r_s parameter mainly as a plotting variable in the figures, and not for any many-body calculations. Hence a choice of r_s, which differs from that used in our work by a factor of ~ 1.49, is immaterial. In the review article by Kravchenko and Sarachik,[1] values of r_s are further modified by the experimentally obtained m^* to discuss the interactions in Si MOSFETs. Thus their r_s^* is explicitly modified to serve a specific purpose. Das Sarma and Hawang[28] have also examined Si-MOSFET resistivities, using an impurity-scattering calculation which requires defining the effective background dielectric constant. They point out that their results are qualitative. Their results would not be affected by the choice of either formula given by Ref. 2, i.e, using $\bar{\epsilon}=7.7$ or 11.5. Altshuler and Maslov[29] actually consider the implications of the suboxide layer and how this could play a significant role in the theory. However, they too point out that their effort is essentially to indicate a "mechanism" rather than a theory of the metal-insulator physics of Si MOSFETs. Hence, once again, the results are too qualitative to make any difference. Similarly, the results of other workers[30] also do not discriminate sufficiently to make the choice of $\bar{\epsilon}$ a significant issue.

Another class of problems where the choice of the average dielectric constant is an issue is in calculating electric subband energies.[2] Although the eigenvalues of the Kohn-Sham equation are not to be considered as effective excitation energies, such an assumption is often made. The input dielectric constant (which decides the effective r_s) enters into the exchange-correlation functions as well as the Poisson potential used. Most calculations are in the high-density regime, and it turns out that, given the uncertainties of the quantum-well potentials and other parameters, the results can be equally well explained by a range of values of the effective dielectric constant.

This situation becomes quite different when it comes to *quantitative* calculations for *low-density* MOSFETs, e.g., in the regime $n=1\times 10^{11}$ electrons/cm^2. Our CHNC calculations for m^* and g^* presented in Ref. 3 and Fig. 4 clearly favor the first formula, Eq. 38 of Ando *et al.*,[2] as the correct formula. This is also the formula that is consistent with the Car-Parrinello optimized atomic structure of the Si/SiO_2 interface obtained from the calculations of Carrier *et al.*[23] and also of Pasquerello *et al.*[25] We believe that the problem of the correct dielectric constant at the Si/SiO_2 interface has received little scrutiny within the 2D electron community in the past, because there was no analytic many-body theory capable of giving quantitative results for low-density electron systems. Also, it is interesting to note that if the second formula of Ando *et al.* were used instead of the first formula that we recommend, then the calculated *total* r_s is close to the $n/2$ value (per valley, $\sim 1.414 r_s$) of r_s calculated by the first formula. This is consistent with the calculations that we advocate, at the Hartree-Fock level (i.e, at the single-electron level). This fact can also lead to some confusion in assessing the validity of numerical calculations.

The CHNC programs for electron-gas calculations mentioned here and in Ref. 7 may be accessed via the internet at the address given in Ref. 31.

V. CONCLUSIONS

We draw the following conclusions from this study. The CHNC method applied to a four-component electron fluid gives results in very close agreement with available diffusion Monte Carlo calculations, without the use of any adjustable parameters specific to the two-valley problem. The ground state of the two-valley 2DES is the unpolarized phase for all r_s, and hence, there is no spin-polarization transition, in contrast to the one-valley 2DES. The coupled-mode approach to constructing the two-valley properties from one-valley data is also fully confirmed. The calculation of the spin-susceptibility enhancement χ_s/χ_P from the second ζ derivative of the spin-dependent energy is found to be very sensitive to the energy difference between the polarized and unpolarized phases and to the form of the polarization dependence. Errors in the assignment of the r_s parameter also plays an increasing role for large r_s. The idealized theoretical 2DES models ignore layer thickness and impurity effects, and yet seem to be within $\sim 2\% - 3\%$ of the experimental results for the susceptibility enhancement. The coupled-

mode form is very successful in capturing the required physics. Thus the QMC, the two-valley CHNC, and the coupled-mode approach based on the one-valley data, provide three independent methods for the study of the strongly coupled 2DES in Si MOSFETs. Finally, we note that the methods used in this paper can be used to study bilayers of electrons and/or holes which are separated by a physical distance d_L, the present work being for $d_L=0$.

*Electronic address: chandre@babylon.phy.nrc.ca
†NRC visiting scientist program.

[1] S. V. Kravchenko and M. P. Sarachik, Rep. Prog. Phys. **67**, 1 (2004).
[2] See, T. Ando, B. Fowler, and F. Stern, Rev. Mod. Phys. **54**, 437 (1982).
[3] M. W. C. Dharma-wardana, cond-mat/0307153.
[4] A. A. Shashkin, M. Rashmi, S. Anissimova, S. V. Kravchenko, V. T. Dolgopolov, and T. M. Klapwijk, Phys. Rev. Lett. **91**, 046403 (2003).
[5] J. Zhu, H. L. Stormer, L. N. Pfeiffer, K. W. Baldwin, and K. W. West, Phys. Rev. Lett. **90**, 056805 (2003).
[6] V. M. Pudalov, A. Punnoose, G. Brunthalef, A. Prinz, and G. Bauer, cond-mat/0104347.
[7] F. Perrot and M. W. C. Dharma-wardana, Phys. Rev. Lett. **87**, 206404 (2001).
[8] N. Q. Khanh and H. Totsuji, Solid State Commun. **129**, 37 (2004).
[9] C. Bulutay and B. Tanatar, Phys. Rev. B **65**, 195116 (2002).
[10] S. Conti and G. Senatore, Europhys. Lett. **36**, 695 (1996).
[11] F. Rapisarda and G. Senatore, Aust. J. Phys. **49**, 161 (1996).
[12] B. Tanatar and D. M. Ceperley, Phys. Rev. B **39**, 5005 (1989).
[13] G. Senatore (private communication) has informed the first author that their results, as presented in Ref. 10, are in agreement with our conclusions.
[14] M. W. C. Dharma-wardana and F. Perrot, Phys. Rev. Lett. **84**, 959 (2000); F. Perrot and M. W. C. Dharma-wardana, Phys. Rev. B **62**, 14766 (2000).
[15] M. W. C. Dharma-wardana and F. Perrot, Phys. Rev. Lett. **90**, 136601 (2003).
[16] M. W. C. Dharma-wardana and F. Perrot, Phys. Rev. B **66**, 014110 (2002).
[17] e.g., G. E. Santoro and G. F. Giulliani, Phys. Rev. B **37**, 4813 (1988). Thus their "antisymmetric" G_- is G_s-1 in our notation.
[18] N. Iwamoto, Phys. Rev. A **30**, 3289 (1984).
[19] P. Vashishta, P. Bhattacharya, and K. S. Singwi, Phys. Rev. B **10**, 5108 (1974); S. Ichimaru, S. Mitake, S. Tanaka, and X.-Z. Yan, Phys. Rev. A **32**, 1768 (1985).
[20] C. Attaccalite, S. Moroni, P. Gori-Giorgi, and G. B. Bachelet, Phys. Rev. Lett. **88**, 256601 (2002).
[21] Y. P. Shkolnikov, K. Vakili, E. P. De Poortere, and M. Shayegan, cond-mat/0402399.
[22] K. Vakili, Y. P. Shkolnikov, E. Tutuc, E. P. de Poortere, and M. Shayegan, cond-mat/0403191.
[23] P. Carrier, L. Lewis, and M. W. C. Dharma-wardana, Phys. Rev. B **65**, 165339 (2002); **64**, 195330 (2001).
[24] N. Tit and M. W. C. Dharma-wardana, J. Appl. Phys. **l86**, 387 (1999).
[25] A. Pasquarello, M. S. Hybertsen, and R. Car, Appl. Surf. Sci. **104/105**, 317 (1996); Appl. Phys. Lett. **68**, 625 (1996).
[26] V. M. Pudalov, M. E. Gershenson, H. Kojima, N. Butch, E. M. Dizhur, G. Brunthaler, A. Prinz, and G. Bauer, Phys. Rev. Lett. **88**, 196404 (2002).
[27] T. Okamoto, K. Hosoya, S. Kawaji, and A. Yagi, Phys. Rev. Lett. **82**, 3875 (1999).
[28] S. Das Sarma and E. H. Hwang, Phys. Rev. Lett. **83**, 164 (1999).
[29] B. L. Altshuler and D. L. Maslov, Phys. Rev. Lett. **82**, 145 (1999).
[30] A. Punnoose and A. M. Finkelstein, Phys. Rev. Lett. **88**, 016802 (2002).
[31] http://babylon.phy.nrc.ca/ims/qp/chandre/chnc